BEHAVIOR OF CONTINUOUS CASTING FLUXES DURING HEATING AND COOLING [1]

Elena Brandaleze [2]
Lucas Castellá [2]
Edgardo Benavidez [3]

Summary

The knowledge of the physical and chemical properties as well as the behaviour of the mould fluxes during melting are important in order to improve continuous casting operations. Lubrication and control of heat transfer in the mould are the more relevant functions of these materials. Values of physical properties like viscosity and surface tension at melting range temperatures are required, as much as the thermal behaviour under process conditions.

The heat extraction from the liquid steel has an important effect in the final quality of products. Mould fluxes are constituted by different oxides, and may form glasses and crystal phases during cooling. The solidification rate and the chemical composition determine the proportion, type and crystalline morphology, which are responsible of the thermal transfer processes.

In this paper, viscosity values are reported in the melting range temperatures calculated by means of the Riboud model and compared with fluidity results obtained by inclined plane technique. Also the linear expansion of the mould fluxes at high temperatures was determined by dilatometry. The crystallization in two different fluxes were determined by DTA tests and correlated with the basicity index. Crystal phases were evaluated by scanning electronic microscopy on quenched samples at 1300 °C. This information is relevant to increase the knowledge on peritectic steel grades casting process in order to improve its quality.

Key words: mould fluxes, heat transfer, peritectic steels.

_____

1. INTRODUCTION

In the continuous casting process the molten steel is delivered through a submerged entry nozzle into a mould. The steel against the mould freezes; the shell is formed. Mould fluxes are placed on the top of the liquid steel to bring lubrication and to control heat transfer process.

Sticking and cracking phenomenon are particular problems determined by the interruption of the molten slag flow. As a consequence, thermal stresses in the shell appeared and are the results of different thermal contraction coefficients between ferrite and austenite phases. A high value of heat flow is related with surface defects, especially for peritectic steel grades. Therefore the knowledge of the amount of crystal phases in the slag film is a fundamental step in the developing or mould flux selection in connection with these steel grades and operating parameters.

Recent literature has focused the attention on the properties of solidifying liquid slag. Nevertheless, traditional data on melting behaviour of mould fluxes as softening, melting and flowing point are relevant and constitute a complementary knowledge to understand the key parameters to control strand lubrication and heat flow between the strand and mould wall.

This paper is focused to study the relation between basicity, the amount of crystal phases, thermal properties and heat transfer referred to slabs casting in peritectic grades.

2. EXPERIMENTAL

Two different mould fluxes, A and B, selected for this study, are used in peritectic grades casting process. The chemical compositions of both fluxes are presented in the Table 1.

Composition (%)	Mould Fluxes	
	A	B
SiO_2	30.50	32.60
CaO	33.50	41.10
Al_2O_3	6.30	3.70
MgO	1.04	2.70
MnO	0.03	-
TiO_2	0.01	0.1
K_2O	0.12	0.06
Fe_2O_3	1.14	0.54
Na_2O	6.80	5.50
F	7.20	7.85
Free C	7.91	3.78

Table 1. Chemical composition of the mould fluxes type A and B.

Another relevant data for the melting fluxes behaviour are the critical temperatures. The fusibility of both powders was measured by Leco (AF-500) instrument. Powders were prepared with a few drops of 10% solution of dextrin containing 0.1% salicylic acid as a preservative. These blends were pressed into a cone mould using a spatula. The cones dried were removed from the mould and the critical temperatures: initial temperature (T_i), softening point (T_s), hemispherical point (T_h), and fluid point (T_f), were determined.

The fluidity of both mould fluxes was determined by means of the inclined plane technique developed by Mills [1]. Samples of 10 g were melted in a platinum crucible up to 1300 °C, after 15 min of maintenance at this temperature they were poured over a plane inclined 10 degrees. The longitude of the mould flux layer formed was measured by a caliber. Averages of several tests were considered in this work to correlate with basicity, physical and thermal properties. The layers obtained, were cut and prepared to carry out a dilatometry test.

Cross sections of the solidified layers were prepared for microscopy observation. To enhance the observation of crystal phases, all the samples were attacked with nital. Because of the high proportion of vitreous phase observed in both types of materials, a second attack with FH acid was carried out. The study by an electronic microscope Philips 505, let us to identify crystal phases and determine the chemical composition using EDS.

The dilatometries were carried out by an horizontal Theta Dilatronic II equipment. Samples with longitudes between 10 to 20 mm were tested. Heating rate was 10 ºC/min. It is important to mention that the test was carried out up to the temperature at which a contraction of the sample was observed.

Simultaneous DTA-TG measurements by a Netzsch STA 409/c analyzer were carried out on samples of 200 mg of each mould flux. A normal atmosphere and a temperature range between room temperature and 1255ºC were used. The fluxes were tested in a Pt-Rh crucible and alumina was used as a reference material. The heating rate selected was 10ºC/min and the cooling rate of 5ºC/min.

3. RESULTS

3.1 Properties related to the chemical composition

According to the mould flux compositions some properties were calculated. Table II show the binary index (CaO/SiO$_2$) and basicity index (Bi) calculated by the equation 1 [2].

$$B_i = \frac{1.53\%\,CaO + 1.51\%\,MgO + 1.94\%\,Na_2O + 3.55\%\,Li_2O + 1.53\%\,CaF_2}{1.48\%\,SiO_2 + 0.10\%\,Al_2O_3} \qquad [1]$$

Viscosity at 1300 ºC were obtained by Riboud model [3] and the system conductivity (K_{sys}) of each mould flux was obtained according to Holzhauser et al [4]. These values are presented in the Table 2. Critical temperatures corresponding to A and B fluxes are also shown in Table 2.

Properties		Mould Fluxes	
		A	B
Binary basicity index		1.09	1.26
Basicity B_i (Branion)[2]		1.77	1.68
Viscosity at 1300ºC (Riboud)[3] (dPa.s)		1.15	0.62
Long. inclined plane, 1300ºC (mm)		32.2	34.8
K_{sys} System conductivity[4] ($Wm^{-1}K^{-1}$)		1.10	1.16
Critical temperatures	IT ºC	1097	1181
	ST ºC	1130	1184
	HT ºC	1147	1198
	FT ºC	1157	1218

Table 2. Values of basicity, viscosity and system thermal conductivity.

3.2 Differential Thermal Analysis and Thermogravimetry

DTA-TG heating curves for the mould flux A are presented in Figure 1. As it is possible to observe, an exothermic peak appears at 410 º C for this material. From this temperature up to 840 º C a series of exothermic reactions occur accompanied by a mass loss. In the range between 410 – 840 º C the weight loss is 12.3 %. At higher temperatures the mass of material remains without changes. Deriving the TG-curve (curve DTG in Figure 1) three peaks can be identified at the following temperatures: 495 º C, 557 º C and 722 º C. Therefore, at these temperatures the highest rates of mass loss are presented. At higher temperatures than 1000 º C, the DTA-curve presents two small endothermic peaks.
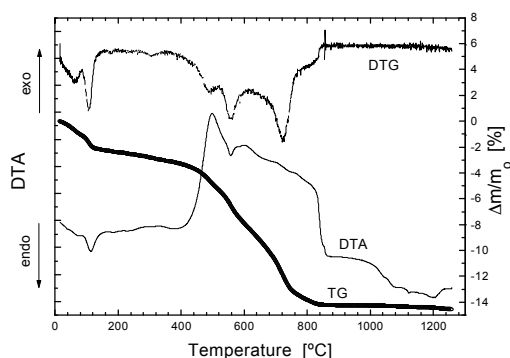

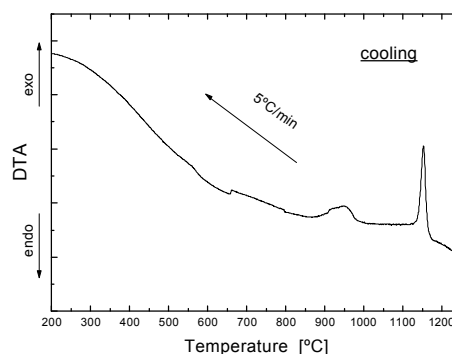Figure 1. DTA–TG Curves for the mould flux A

Figure 2. DTA cooling curve for the mould flux A

DTA cooling curve (Figure 2) shows two exothermic peaks, the first one at 1153ºC and the second one at 946 º C. Throughout the cooling period of mould flux A, the weight remains constant (not shown in the Figure 2).

The curves of DTA-TG corresponding to the heating of the mould powder B are presented in Figure 3. In this case, the exothermic reactions take place from 150 º C to 780 º C. Four peaks were clearly identified in the DTA curve. These reactions are coincident with an increase in the loss mass rate (curve DTG) and they are

accompanied by a continuous lost of weight. At higher temperatures a neglected weight loss (approx. 0.5%) took place.
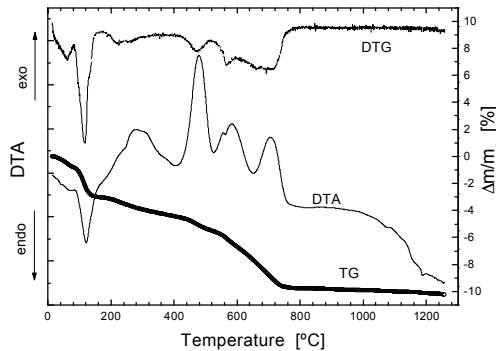

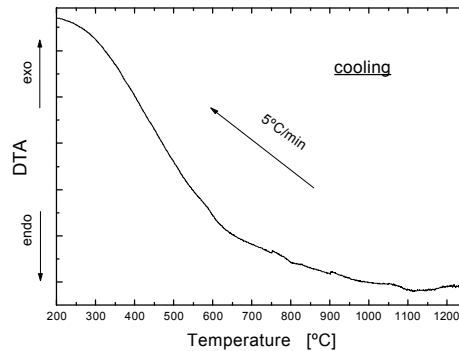Figure 3. DTA–TG Curves for the mould flux B

Figure 4. DTA cooling curve for the mould flux B

The cooling cycle of sample B, not presents exothermic peaks indicating any crystallization reaction. Similar to the sample A, there is no change in the weight during the cooling of sample B (not shown in Figure 4).

3.3 Dilatometric analysis

Dilatometric runs were carried out on samples A and B, the linear expansion coefficient (α) can be calculated. The α values corresponding to samples A and B are shown in Figure 5. A smaller value of the linear expansion coefficient of sample A is observed throughout the temperature range analysed.
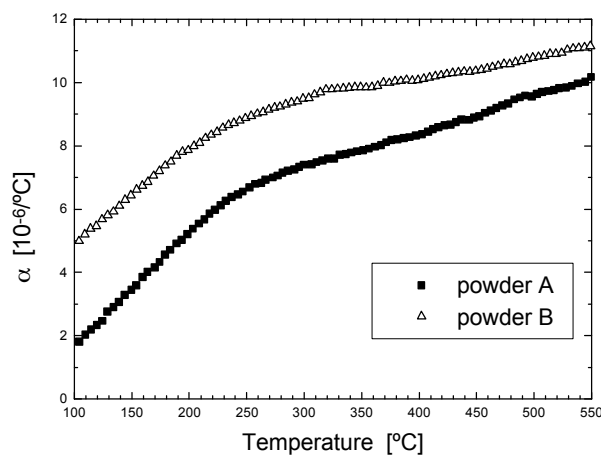

Figure 5. Linear expansion coefficient of sample A and B.

As it is possible to see, both mould fluxes have linear expansion coefficient values that increase continuously during the heating. At first, up to 250 º C, the values of α increase rapidly, and then between 250 – 550ºC they increase more gradually. At temperatures higher than 545 º C for the sample A (and 575ºC for the sample B), the dilatometric curve suffer an important increase in its expansion rate. This anomalous behaviour is associated to the glass transition temperature (T_g) of the vitreous phase present in both samples [5].

3.4. Electronic microscopy

SEM studies on mould flux A sample, permit to determine a large amount of vitreous phase. A thin dendrite crystal layer was formed in a localised area of the sample surface. A general microstructure of the crystalline and glass phases is observed in Figure 6.
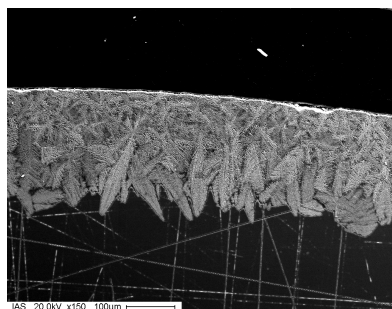

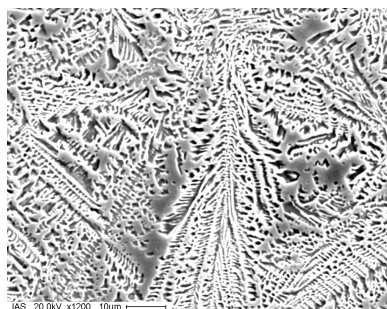Figure 6. Aspect of the A flux general microstructure. [150x]

Figure 7. Dendrite detail. [1200x]

In Figure 7, dendrite crystal details are observed. Chemical composition of the dendrite crystal (D) and the interdendritic liquid (I) were determined by EDS; results are shown in table 3.

Material A	Na_2O (%)	MgO (%)	Al_2O_3 (%)	SiO_2 (%)	CaO (%)	FeO (%)
I	6.0	-	12.9	48.7	31.1	1.3
D	7.2	3.3	14.2	50.0	24.2	-

Table 3. Dendrite and interdendritic liquid chemical composition of the material A.

Maps corresponding to Al, Ca and Si elements are presented in Figure 8.

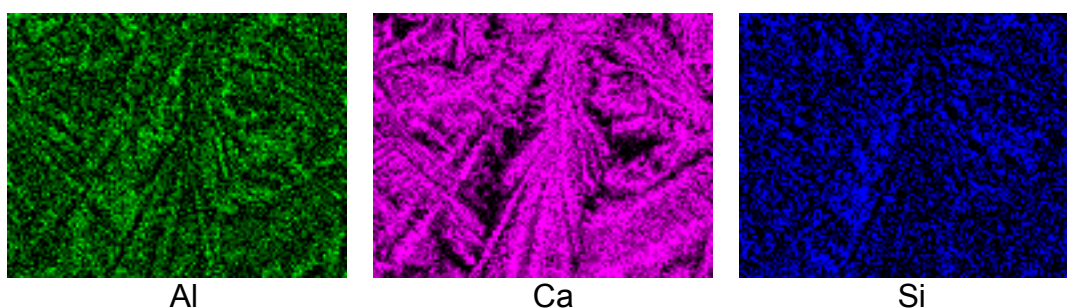Al   Ca   Si

Figure 8. Maps of the elements present in the crystal phases of A material.

In material B, more vitreous phase without crystalline layer was formed, only isolated crystals next to the surface were observed as it is shown in Figure 9.
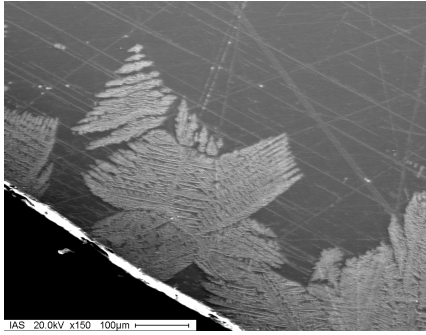
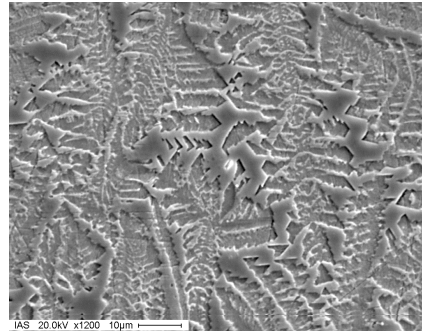Figure 9. Aspect of the B flux general microstructure. [150x]

Figure 10. Dendrite detail. [1200x]

The dendrite morphology is shown in Figure 10. The chemical analysis of dendrite and interdendritic zones were analysed by SEM/EDS and they are present in Table 4.

Material B	Na_2O (%)	MgO (%)	Al_2O_3 (%)	SiO_2 (%)	CaO (%)	FeO (%)
I	-	-	5.5	47.7	46.2	0.64
D	5.1	6.3	10.1	53.8	25.5	-

Table 4. Dendrite and interdendritic liquid chemical composition of the material B.

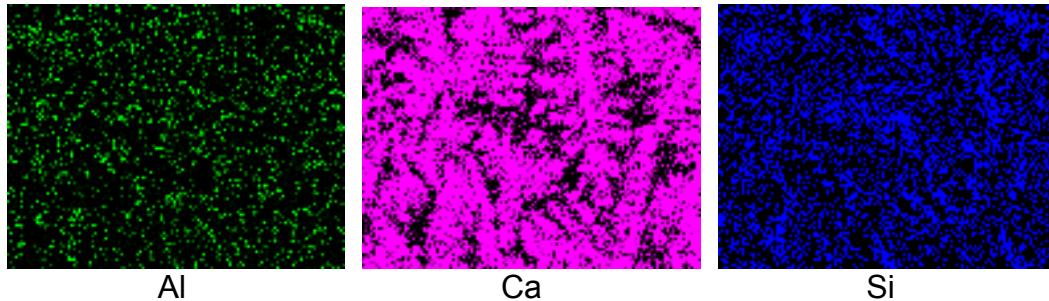Maps of Al, Ca and Si of the crystal can be observed in the Figure 11.

Al

Ca

Si

Figure 11. Maps of the elements present in the crystals of B material.

4. DISCUSSION

The heat flow balance and the lubrication effect in the continuous casting process are the major problems for medium C, low C and peritectic steel grades. The precipitation of crystalline phases whose proportion increases with basicity [6] causes thermal heterogeneity and bad lubrication. According to the values of binary basicity, large amount of vitreous phase should be developed in both powders. However, values of the B_i basicity obtained contemplates the whole chemical composition and permit to think that the crystallising tendency will be higher in the mould flux A than in B.

According to SEM observations, flux B presents a very low proportion of crystalline phase, which is confirmed, for the crystallisation peaks obtained during its cooling cycle by DTA. This material presents small, isolated and dispersed crystals on the surface. The higher proportion of vitreous phase promotes the radiation heat transfer contribution and the conduction by phonon mechanism can be neglected.

Although the powder A presented crystallisation peaks during its cooling cycle, the microstructure observations showed also a scarce presence of crystals. However, in this sample the crystals were detected in more proportion than in B. At high temperatures, the heat transfer by radiation mechanism prevails on that by conduction one. According to these results, the conduction component of heat transfer would not be important in both samples. This fact permits to think that, in the initial instants of the process, the slab will freeze rapidly using the material A as well as B.

It is known that peritectic steels are susceptible to cracking. In general these cracks are generated because of thermal stress generated in the shell, resulting from differences in thermal contraction between ferrite and austenite phases [7]. Differential contractions promote the early separation between metal and mould, that it can be reverted through a thicker mould powder layer but with a low viscosity [5].

Both powders have low viscosity at 1300 º C and the smaller value is for powder B. The viscosity, calculated in theoretical form can be experimentally confirmed by the inclined plane tests. A longer layer confirmed a higher fluidity for the powder B. Also, the lower linear expansion coefficient of the material A (α) indicates that this material has a structure that does not allow an easy displacement of the SiO_4 [2]⁻ tethraedra. At higher temperature, when the powder is molten, this structure means a higher viscosity. This finding is consistent with the binary index but not with the Bi index.

The penetration of the liquid slag and the thickness of the formed layer between the shell and the mould (d_{cf}) are factors that have influence in the lubrication process during the steel casting. These conditions are largely dependent from the viscosity of the mould fluxes at high temperatures. It is known that a higher viscosity generates a thicker layer of fluxes when they are flowing between the shell and the mould. Due the smaller viscosity of the powder B than of the powder A, it should be expected that the layer formed by the powder B is thinner. Also, the thermal conductivity of the system calculated to the powder B, $k_{sys}(B)$, is higher than k_{sys} (A). Therefore, using the expression to heat flow [7] $q = (k_{sys}/d_{cf})$, (at T_m), it is expected that the heat extraction would be faster with the material B.

According to the relationship [7] : $\eta.Vc \approx 2$ is advisable that the mould flux B should be casting at more rate than the A. The higher casting rate associated to mould fluxes B is also possible to realise because this powder B allows a higher speed of heat extraction.

5. CONCLUSIONS

Dilatometric assays and inclined plane test demonstrated to be useful to confirm calculated fluidity and viscosity.

A higher crystallization grade was determined in the powder A from DTA runs and microstructural observations.

From the obtained results in this work it can be inferred that both powders A and B can be used in continuous casting of peritectic steel slabs, taking into account that a higher casting speed for the mould powder B should be considered.

REFERENCES

1. Mills, K.C., Halali M., Lörz H.P., et all., A Simple test for the measurement of slag viscosities. 5th Conference on Molten Slags, Fluxes and Salts, 1997, pp. 535 – 542.

2. Branion R.V., Mold Fluxes for Continuous Casting, *Iron and Steelmaking, 1986, September*, pp. 41 – 50.

3. Riboud P. V., Continuous casting slags. Seminaire: Formation de la première peau en coulée continue, Institut de Recherches de la Sidérurgie Française IRSID, 1985, pp. 1 – 30.

4. Holzhauser J.F., Spitzer K.H. and Schwerdtfeger K. Study of heat transfer through layers of casting flux: experiments with a laboratory set – up simulating the conditions in continuous casting. *Steel Research*, vol 70, no. 7 1999. pp. 252 – 258.

5. J. Hlavac, The technology of glass and ceramics: An introduction, Elsevier Scientific Publishing Company, New York (1983).

6. Carli R. and Ghilardi V., Managing Technological Properties of mold Fluxes, *Iron and Steelmaking, 1998,* pp. 43 – 46.

7. Chávez J.F., Rodríguez A., Morales R. and Tapia V., Laboratory and Plant studies on thermal properties of Mold Powders. *Steelmaking Conference,* 1995, pp. 679 – 686.

8. Mills K.C. and Fox A.B. Mould Fluxes, *Mills Symposium,* V 1, London, 2002.